IEEE Access
Multidisciplinary | Rapid Review | Open Access Journal

Received April 1, 2019, accepted April 11, 2019, date of publication April 22, 2019, date of current version May 2, 2019.

Digital Object Identifier 10.1109/ACCESS.2019.2912402

Covariance Matrix Reconstruction via Residual Noise Elimination and Interference Powers Estimation for Robust Adaptive Beamforming

XINGYU ZHU, ZHONGFU YE, XU XU, AND RUI ZHENG

Department of Electronic Engineering and Information Science, University of Science and Technology of China, Hefei 230027, China
National Engineering Laboratory for Speech and Language Information Processing, Hefei 230027, China

Corresponding author: Zhongfu Ye (yezf@ustc.edu.cn)

This work was supported in part by the National Natural Science Foundation of China under Grant 61671418, and in part by the Advanced Research Fund of the University of Science and Technology of China.

ABSTRACT Recently, a number of robust adaptive beamforming (RAB) methods based on Capon power spectrum estimator integrated over a specific region for covariance matrix reconstruction have been proposed. However, all of these methods ignore the residual noise existing in the Capon spectrum estimator, which results in reconstruction errors. In this paper, we propose a RAB algorithm via residual noise elimination and interference powers estimation to reconstruct covariance matrix. First, the proposed algorithm demonstrates the existence of residual noise and analyze its relationship to actual noise. Then, after eliminating the residual noise, the modified Capon power spectrum estimator is utilized to reconstruct the covariance matrix and desired signal SV. Moreover, to reduce the influence of the desired signal on interference powers estimation, we project the snapshots onto the complementary subspace of the desired signal and estimated interference powers are derived according to the theoretical formulation of the interference covariance matrix (ICM). The simulation results demonstrate that the proposed method is robust against various mismatches and can achieve superior performance.

INDEX TERMS Robust adaptive beamforming (RAB), steering vector (SV) estimation, powers estimation, covariance matrix reconstruction.

I. INTRODUCTION

Adaptive array signal processing is one of the major areas in signals and has been studied extensively because it's widely applied in many fields such as radar, sonar, wireless communication, speech processing, biomedicine, radio astronomy, etc. It involves multiple sensors placed at different positions in space to process the received signals impinging from different directions. As an important branch of array signal processing, the adaptive beamfroming adjusts its weight vector depend on the environment to enhance the desired signal and suppress the interferences and noise, where it can be regarded as a spatial filtering technique. The standard Capon beamforming [1] is an optimal adaptive beamforming when the precise knowledge of desired signal is available and the covariance matrix of received is exactly known, the Capon beamformer can yield both excellent output performance and high convergence rate. However, the standard adaptive beamforming [1] is sensitive to mismatch errors such as signal direction errors, sensor position errors, amplitude and phase errors and so on, especially when the desired signal components is present in the sample covariance matrix, and these could result in performance degradation [2], [3]. Therefore, the robustness of adaptive beamforming has become the focus of research.

To improve the robustness of the adaptive beamforming, many technologies have been proposed, and they can be classified as following categories: diagonal loading (DL) technologies [4]–[7], Eigenspace-based technologies [8]–[12], uncertainty set constraint technologies [13]–[17] and covariance matrix reconstruction technologies [18]–[23]. DL [4] technologies are widely used to improve the robustness by adding a scaled identity matrix to the sample covariance matrix. Unfortunately, it's difficult to choose the optimal DL factor in practice. In [7], the DL factor can be automatically computed but this method fails to provide

The associate editor coordinating the review of this manuscript and approving it for publication was Mohammad Zia Ur Rahman.

satisfactory performance in high input signal to noise ratios (SNRs). Eigenspace-based [8] technologies are implemented by projecting the nominal steering vector (SV) onto the signal plus interference subspace. However the performance of Eigenspace-based beamformers degrade drastically at low input SNRs, where the signal subspace may be swapped with noise subspace. The main idea of uncertainty set constraint algorithms [13] is to constrain the SV on the presumed spherical or ellipsoidal and SV is estimated by solving a second-order cone programming problem with high computational complexity. Moreover, uncertainty set constraint algorithms have been proven to be equivalent to the DL algorithms.

In order to remove the desired signal components from sample covariance matrix, nowadays, a number of algorithms based on interference-plus-noise covariance matrix (INCM) reconstruction have become popular. The authors of [18] firstly employ Capon spatial power spectrum estimator integrating over the regions separated from desired signal to reconstruct INCM. The method in [19] modifies the linear integration area [18] into annulus uncertainty set to reconstruct INCM, which has the obvious performance improvement but with high computational complexity. Both in [18], [19], the desired signal SV is obtained by solving a quadratically constrained quadratic programming (QCQP) problem. To reduce the computational complexity, a spatial power spectrum sampling method is proposed in [20], it requires large number of sensors to achieve the comparable performance as [18]. In [22], INCM is reconstructed by searching for the interference SVs lying in the intersection of two subspaces, however one of subspaces is the reconstructed INCM in [18]. Besides, it also need Eigen-decomposition several times depending on the number of interference. Nonetheless, all these methods ignore the influence of residual noise on covariance matrix reconstruction, which would lead to reconstruction errors. The authors of [23] propose a novel reconstruction method by estimating all interference SVs and corresponding powers, whereas the estimated powers are based on the approximately orthogonality of different SVs rather than strictly orthogonal. In addition, the sample covariance matrix is used to compute the interference powers, where the desired signal is existed in the sample covariance matrix and it may cause estimation errors.

This paper focuses on improving the performance of adaptive beamformers when mismatch errors are existed. Different from the previous INCM reconstruction methods. In this paper, a novel RAB algorithm based on the residual noise elimination and interference powers estimation is developed. Analyzed from [18], [19], [22], the performance of INCM reconstruction methods depend on the accuracy of covariance matrix reconstruction. Compared with [18], the reconstruction method in [19] narrows the integral regions to reduce the useless information. And in [22], the reconstructed INCM is the linear combination of interference SVs and associated powers, which contains the less redundant information. Thus, we exploit a more effective way to improve the accuracy of SV and covariance matrix to resist various mismatch errors. The proposed algorithm demonstrates the existence of residual noise and analyze its numerical changes to calculate the actual noise power, and we can reduce reconstruction errors of desired signal covariance matrix reconstruction by eliminating the residual noise. The prime eigenvector of reconstructed desired signal covariance matrix containing the most information is regarded as the desired signal SV. In order to reduce the influence of desired signal on interference powers estimation, we project the snapshots onto the complementary subspace of desired signal. Then we derive the estimated interference powers based on the theoretical formulation of interference covariance matrix (ICM). Simulation results show that the proposed algorithm has better performance in terms of robustness and output signal-to-interference-plus-noise ratio (SINR) in most cases of mismatches comparing with other existing methods.

The main contributions of our work are summarized as follows:

- A RAB algorithm based on residual noise elimination and interference powers estimation is developed. We demonstrate the existence of residual noise and analyze its relationship to actual noise.
- The desired signal SV is estimated from the reconstructed covariance matrix which doesn't suffer from the influence of residual noise.
- The estimated interference powers are derived depending on the theoretical ICM expression and we reconstruct the ICM as theoretical formulation.

The rest of this paper is organized as follows. The signal model and necessary background about adaptive beamforming technology are introduced in section II. In section III, the proposed RAB algorithm is described in detail and the analysis of performance is performed. The simulation results are provided in section IV. Finally, conclusions are drawn in Section V.

II. PROBLEM BACKGROUND

Consider a uniform linear array (ULA) composed of M omnidirectional sensors that receives $L+1$ uncorrelated narrowband signals from far-field sources. All signals are uncorrelated with noise. The $M \times 1$ complex array observation vector at time k is modeled as:

$$\mathbf{x}(k) = \mathbf{x}_s(k) + \mathbf{x}_i(k) + \mathbf{x}_n(k) \tag{1}$$

where $\mathbf{x}_s(k) = s_0(k)\mathbf{a}_0$, $\mathbf{x}_i(k) = \sum_{l=1}^{L} s_l(k)\mathbf{a}_l$ and $\mathbf{x}_n(k)$ stand for the components of desired signal, interference and noise, respectively. $s_l(k)$ and $\mathbf{a}_l$, $l = 0, 1, \cdots, L$ are the l-th signal waveform and corresponding SV, respectively. $\mathbf{x}_n(k)$ is the additive Gaussian noise with zero mean and equal variance. The SV of ULA has the following general form:

$$\mathbf{a}(\theta) = [1, e^{-j2\pi \frac{d\sin\theta}{\lambda}}, \cdots, e^{-j2\pi \frac{(M-1)d\sin\theta}{\lambda}}]^T \tag{2}$$

where d is the distance between two adjacent sensors and λ is the wavelength of sources and θ is the angle between

the incident signal and the array normals. $(\cdot)^T$ denotes the transpose. Apparently, the Euclidean norm of steering vector is $\sqrt{M}$:

$$\|\mathbf{a}\|_2^2 = M \tag{3}$$

where $\|\cdot\|_2$ denotes the ℓ_2 norm. The output of beamformer is written as:

$$y(k) = \mathbf{w}^H \mathbf{x}(k) \tag{4}$$

where $\mathbf{w} = [w_1, w_2, \cdots, w_M]^T$ is the complex weight vector of beamformer and $(\cdot)^H$ denotes the Hermitian transpose. The optimal weight vector $\mathbf{w}$ is solved by maximizing the output SINR:

$$\boldsymbol{SINR} = \frac{\sigma_s^2 |\mathbf{w}^H \mathbf{a}_0|^2}{\mathbf{w}^H \mathbf{R}_{i+n} \mathbf{w}} \tag{5}$$

where $\sigma_s^2 = E\{|s_0(k)|^2\}$ denotes the power of desired signal and $E\{\cdot\}$ stands for the expectation operator of stochastic variables. $\mathbf{R}_{i+n}$ is the theoretical INCM expressed as:

$$\begin{aligned} \mathbf{R}_{i+n} &= E\{(\mathbf{x}_i(k) + \mathbf{x}_n(k))(\mathbf{x}_i(k) + \mathbf{x}_n(k))^H\} \\ &= \sum_{l=1}^{L} \sigma_l^2 \mathbf{a}_l \mathbf{a}_l^H + E\{\mathbf{x}_n(k)\mathbf{x}_n^H(k)\} \\ &= \mathbf{R}_i + \sigma_n^2 \mathbf{I} \end{aligned} \tag{6}$$

where σ_l^2, σ_n^2, $\mathbf{R}_i$ and $\mathbf{I}$ represent the l-th interference power, noise power, theoretical ICM and identity matrix, respectively. The maximization of the output SINR is formed as:

$$\min_{\mathbf{w}} \ \mathbf{w}^H \mathbf{R}_{i+n} \mathbf{w} \quad \textit{subject to } \mathbf{w}^H \mathbf{a}_0 = 1 \tag{7}$$

The above optimization problem is known as minimum variance distortionless respond (MVDR) beamformer and the optimal solution is:

$$\mathbf{w}_{opt} = \frac{\mathbf{R}_{i+n}^{-1} \mathbf{a}_0}{\mathbf{a}_0^H \mathbf{R}_{i+n}^{-1} \mathbf{a}_0} \tag{8}$$

It has been proved that replacing $\mathbf{R}_{i+n}$ by $\mathbf{R}$ doesn't change the optimal output SINR [24], and then (8) changes to the weight of Capon beamformer:

$$\mathbf{w}_{Capon} = \frac{\mathbf{R}^{-1} \mathbf{a}_0}{\mathbf{a}_0^H \mathbf{R}^{-1} \mathbf{a}_0} \tag{9}$$

The output power of the Capon beamformer is obtained:

$$P = \mathbf{w}_{Capon}^H \mathbf{R} \mathbf{w}_{Capon} = \frac{1}{\mathbf{a}_0^H \mathbf{R}^{-1} \mathbf{a}_0} \tag{10}$$

where $\mathbf{R}$ is the theoretical array covariance matrix expressed as:

$$\begin{aligned} \mathbf{R} &= \mathbf{R}_s + \mathbf{R}_{i+n} \\ &= \sigma_s^2 \mathbf{a}_0 \mathbf{a}_0^H + \sum_{l=1}^{L} \sigma_l^2 \mathbf{a}_l \mathbf{a}_l^H + \sigma_n^2 \mathbf{I} \end{aligned} \tag{11}$$

Capon spatial power spectrum [25] is employed as a power estimator over all directions:

$$P(\theta) = \frac{1}{\mathbf{a}^H(\theta) \mathbf{R}^{-1} \mathbf{a}(\theta)} \tag{12}$$

where $\mathbf{a}(\theta)$ is the actual SV associated with a hypothetical direction θ. However, $\mathbf{R}$ and $\mathbf{R}_{i+n}$ are unavailable in practice, and they are usually replaced by the sample covariance matrix $\hat{\mathbf{R}} = \frac{1}{K} \sum_{k=1}^{K} \mathbf{x}(k)\mathbf{x}^H(k)$ with K received snapshots. In addition, the precise array structure is hard to obtain as well, so the compromise is to replace $\mathbf{a}(\theta)$ by the nominal SV $\bar{\mathbf{a}}(\theta)$ based on the known array structure:

$$\hat{P}(\theta) = \frac{1}{\bar{\mathbf{a}}^H(\theta) \hat{\mathbf{R}}^{-1} \bar{\mathbf{a}}(\theta)} \tag{13}$$

correspondingly, the optimal weight vector becomes to the sample covariance inversion (SMI) beamformer:

$$\mathbf{w}_{SMI} = \frac{\hat{\mathbf{R}}^{-1} \bar{\mathbf{a}}_0}{\bar{\mathbf{a}}_0^H \hat{\mathbf{R}}^{-1} \bar{\mathbf{a}}_0} \tag{14}$$

III. PROPOSED METHOD

A. THE ANALYSIS OF RESIDUAL NOISE AND DESIRED SIGNAL SV ESTIMATION

Most of the existing INCM reconstruction methods are based on (12) integrating over the angular sectors. However, they all ignore that the Capon spatial power spectrum estimator (12) contains power of residual noise, where the residual noise would lead to inaccurate reconstruction through integration.

Without loss of generality, assuming that $\mathbf{R}$ only contains complex Gaussian white noise and one signal no matter desired signal or interference, and then it can be expressed as $\mathbf{R} = \sigma^2 \mathbf{a}(\theta_{i1}) \mathbf{a}^H(\theta_{i1}) + \sigma_n^2 \mathbf{I}$, where σ^2 denotes the power of impinging signal and θ_{i1} is the associated direction. Accordingly, (12) changes to:

$$P(\theta) = \frac{1}{\mathbf{a}^H(\theta) \left(\sigma^2 \mathbf{a}(\theta_{i1}) \mathbf{a}^H(\theta_{i1}) + \sigma_n^2 \mathbf{I} \right)^{-1} \mathbf{a}(\theta)} \tag{15}$$

When $\theta = \theta_{i1}$, using the matrix inversion lemma [26], the above equation is rewritten as:

$$\begin{aligned} P(\theta_{i1}) &= \frac{1}{\mathbf{a}^H(\theta_{i1}) \left(\sigma^2 \mathbf{a}(\theta_{i1}) \mathbf{a}^H(\theta_{i1}) + \sigma_n^2 \mathbf{I} \right)^{-1} \mathbf{a}(\theta_{i1})} \\ &= \frac{\sigma_n^2}{M} + \sigma^2 \end{aligned} \tag{16}$$

The (16) implies that in the impinging direction, the power is the sum of residual noise and signal, and the power of residual noise has become $1/M$ of actual noise. We can also verify the existence of residual noise from another aspect. If $\mathbf{R}$ is only comprised of complex Gaussian white noise, it means $\mathbf{R} = \sigma_n^2 \mathbf{I}$. Correspondingly, (12) becomes to:

$$P(\theta) = \frac{1}{\mathbf{a}^H(\theta) (\sigma_n^2 \mathbf{I})^{-1} \mathbf{a}(\theta)} = \frac{\sigma_n^2}{M} \tag{17}$$

(17) demonstrates the existence of residual noise, and the residual noise is distributed in the whole space. So we can infer that in the directions of incident signals, the power is the sum of signal and residual noise, and in the directions away from the regions of signals, only residual noise exists. Fig. 1 is drawn in the condition of $d/\lambda = 1/2$, and it shows the magnitude of power in whole space according to (12), where we set the power of one desired signal and two interference as 0 dBw respectively, and the noise variance is set as $\sigma_n^2 = 1$. It can be seen that in each peak, the magnitude of power is 1.1 which is larger than its actual value and consistent with (16), and in the regions away from impinging signals, the magnitude of power is 0.1 rather than zero, which is consistent with (17).

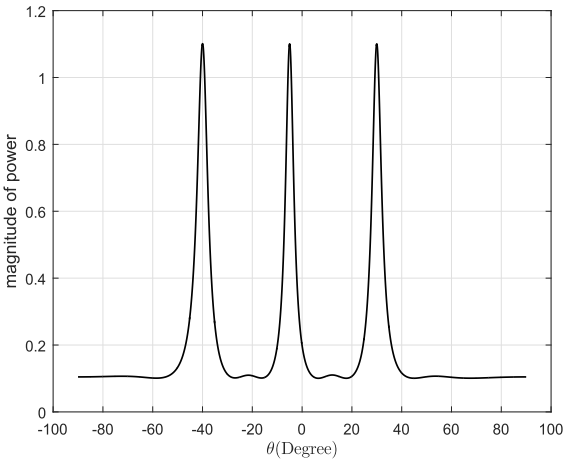

FIGURE 1. Power distribution of one 0 dBw desired signal from −5° and two 0 dBw interference from −40° and 30° with $M = 10$.

Most INCM reconstruction methods employ the equation (13) as follow:

$$\begin{aligned}\bar{\mathbf{R}}_p &= \int_{\Theta_p} \hat{P}(\theta)\bar{\mathbf{a}}(\theta)\bar{\mathbf{a}}^H(\theta)d\theta \\ &= \int_{\Theta_p} \frac{1}{\bar{\mathbf{a}}^H(\theta)\hat{\mathbf{R}}^{-1}\bar{\mathbf{a}}(\theta)}\bar{\mathbf{a}}(\theta)\bar{\mathbf{a}}^H(\theta)d\theta \end{aligned} \tag{18}$$

where Θ_p represents the specific angular sectors. While they all ignore the residual noise components in $\hat{P}(\theta)$, and this would lead to inaccuracy reconstruction because of collecting plenty of redundant components. Although the power of residual noise σ_n^2/M may very small compared with the impinging signals, the influence cannot be ignored after the integration operation.

According to the above analysis, we firstly estimate the residual noise power by average operation:

$$\bar{\sigma}_n^2 = \frac{1}{T}\sum_{t=1}^{T}\frac{1}{\bar{\mathbf{a}}^H(\theta_t)\hat{\mathbf{R}}^{-1}\bar{\mathbf{a}}(\theta_t)}, \quad \theta_t \in \Theta_n \tag{19}$$

where Θ_n is the angular regions separated from desired signal and interference, and θ_t is the discrete sample point in Θ_n. T is the number of sample points. We sum up the powers away from the impinging signal angle regions and then average it, and result is regarded as the residual noise power. Based on this, the actual noise power and noise covariance matrix can be calculated respectively:

$$\hat{\sigma}_n^2 = M\bar{\sigma}_n^2 \tag{20}$$

$$\hat{\mathbf{R}}_n = \hat{\sigma}_n^2\mathbf{I} \tag{21}$$

In order to obtain the estimated SV of desired signal, we need to reconstruct the accurate desired signal covariance matrix. Different from (18), we remove the residual components from $\hat{P}(\theta)$:

$$\begin{aligned}\hat{\mathbf{R}}_s &= \int_{\Theta_s} (\hat{P}(\theta) - \bar{\sigma}_n^2)\bar{\mathbf{a}}(\theta)\bar{\mathbf{a}}^H(\theta)d\theta \\ &= \int_{\Theta_s} (\frac{1}{\bar{\mathbf{a}}^H(\theta)\hat{\mathbf{R}}^{-1}\bar{\mathbf{a}}(\theta)} - \bar{\sigma}_n^2)\bar{\mathbf{a}}(\theta)\bar{\mathbf{a}}^H(\theta)d\theta \\ &= \int_{\Theta_s} \frac{\bar{\mathbf{a}}(\theta)\bar{\mathbf{a}}^H(\theta)}{\bar{\mathbf{a}}^H(\theta)\hat{\mathbf{R}}^{-1}\bar{\mathbf{a}}(\theta)}d\theta - \int_{\Theta_s} \bar{\sigma}_n^2\bar{\mathbf{a}}(\theta)\bar{\mathbf{a}}^H(\theta)d\theta \end{aligned} \tag{22}$$

where Θ_s denotes angular sector of desired signal and $\bar{\Theta}_s$ is the complement angular sector of Θ_s. We should note that the above equation is quite different from diagonal loading method, because the term of $\int_{\Theta_s} \bar{\sigma}_n^2\bar{\mathbf{a}}(\theta)\bar{\mathbf{a}}^H(\theta)d\theta$ stands for the redundant components in $\bar{\Theta}_s$ and is not a diagonal matrix entirely.

The term $\hat{P}(\theta) - \bar{\sigma}_n^2$ stands for the accuracy power distribution of signals, and it should be the positive. So we only choose the positives value of $\hat{P}(\theta) - \bar{\sigma}_n^2$ in Θ_s and ignore the negative values. Moreover, $\bar{\sigma}_n^2$ also can be regarded as the threshold to determine the effective regions of integration, and if $\bar{\sigma}_n^2$ is set larger, the range of Θ_s would be smaller. The prime eigenvector of $\hat{\mathbf{R}}_s$ in (22) contains the most information of desired signal which can be regarded as the estimated SV:

$$\hat{\mathbf{R}}_s = \sum_{m=1}^{M}\alpha_m\mathbf{c}_m\mathbf{c}_m^H \tag{23}$$

where α_m, $m = 1, 2, \cdots, M$ are the eigenvalues of $\hat{\mathbf{R}}_s$ arranged in descending order (i.e. $\alpha_1 \geq \alpha_2 \geq \cdots \geq \alpha_M$), $\mathbf{c}_m$ is the eigenvector corresponding to α_m. The principal eigenvector of $\hat{\mathbf{R}}_s$ covers the most information of desired signal and the rest are residual components. Consequently, the desired signal SV is supposed as follow:

$$\hat{\mathbf{a}}_s = \sqrt{M}\mathbf{c}_1 \tag{24}$$

where $\mathbf{C} = [\mathbf{c}_1, \mathbf{c}_2, \cdots, \mathbf{c}_M] = [\mathbf{C}_1, \mathbf{C}_2]$. $\mathbf{C}_1$ contains N eigenvectors corresponding to N largest eigenvalues. Obviously, $\hat{\mathbf{a}}_s$ belongs to the subspace $\mathbf{C}_1\mathbf{C}_1^H$, and is orthogonal to the complementary subspace of $\mathbf{C}_1\mathbf{C}_1^H$: $\|(\mathbf{I} - \mathbf{C}_1\mathbf{C}_1^H)\hat{\mathbf{a}}_s\|_2 = 0$. This equation can be verified by plotting the value of the term of $\|(\mathbf{I} - \mathbf{C}_1\mathbf{C}_1^H)\bar{\mathbf{a}}(\theta)\|_2^2$. Consider a ULA with $M = 10$ sensors spaced half a wavelength apart, $\Theta_s = [-9°, -1°]$, snapshot $K = 30$, and one 10 dB desired signal from $-5°$ and two 10 dB interference from $-40°$ and $30°$. Fig. 2 depicts the value of $\|(\mathbf{I} - \mathbf{C}_1\mathbf{C}_1^H)\bar{\mathbf{a}}(\theta)\|_2^2$ versus the angle. It can

been seen that when $N = 3$, the term $\|(\mathbf{I} - \mathbf{C}_1\mathbf{C}_1^H)\bar{\mathbf{a}}(\theta)\|_2$ is almost zero for $\forall\theta \in \Theta_s$, and in the complement sector of Θ_s, the $(\mathbf{I} - \mathbf{C}_1\mathbf{C}_1^H)$ hardly changes the norm of SV. So $\|(\mathbf{I} - \mathbf{C}_1\mathbf{C}_1^H)\bar{\mathbf{a}}(\theta)\|$ can be considered as the projection matrix to eliminate desired signal and preserve the interference components.

B. ICM RECONSTRUCTION

For each received snapshot $\mathbf{x}(k)$, the desired signal components is eliminated through projection:

$$\begin{aligned}\tilde{\mathbf{x}}(k) &= \mathbf{P}^H\mathbf{x}(k) \\ &\cong \mathbf{P}^H\mathbf{x}_i(k) + \mathbf{P}^H\mathbf{x}_n(k)\end{aligned} \tag{25}$$

where $\mathbf{P} = \mathbf{P}^H = \mathbf{I} - \mathbf{C}_1\mathbf{C}_1^H$. Then covariance matrix is expressed as:

$$\begin{aligned}\tilde{\mathbf{R}} &= \frac{1}{K}\sum_{k=1}^{K}\tilde{\mathbf{x}}(k)\tilde{\mathbf{x}}^H(k) \\ &= \frac{1}{K}\sum_{k=1}^{K}\mathbf{P}^H\mathbf{x}(k)\mathbf{x}^H(k)\mathbf{P} \\ &= \mathbf{P}^H\hat{\mathbf{R}}\mathbf{P}\end{aligned} \tag{26}$$

The above equation means that the matrix $\tilde{\mathbf{R}}$ is derived from sample covariance matrix $\hat{\mathbf{R}}$ through projection and is absent of desired signal components. We can prove it as follow:

$$\begin{aligned}\tilde{\mathbf{R}} &= \frac{1}{K}\sum_{k=1}^{K}\tilde{\mathbf{x}}(k)\tilde{\mathbf{x}}^H(k) \\ &= \frac{1}{K}\sum_{k=1}^{K}\mathbf{P}^H(\mathbf{x}_i(k) + \mathbf{x}_n(k))(\mathbf{x}_i(k) + \mathbf{x}_n(k))^H\mathbf{P} \\ &\cong \mathbf{P}^H\hat{\mathbf{R}}_i\mathbf{P} + \hat{\sigma}_n^2\mathbf{P}^H\mathbf{P}\end{aligned} \tag{27}$$

The above equation means the matrix $\tilde{\mathbf{R}}$ can be approximated to contain only interference and noise. From Fig. 2, we can see that the projection matrix $\mathbf{P}$ doesn't affect the norm of $\bar{\mathbf{a}}(\theta)$

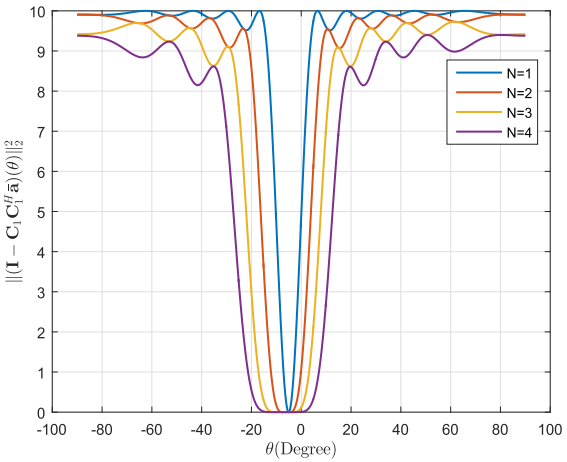

FIGURE 2. Values of $\|(\mathbf{I} - \mathbf{C}_1\mathbf{C}_1^H)\bar{\mathbf{a}}(\theta)\|_2^2$ versus θ.

for $\forall\theta \in \bar{\Theta}_s$, which signifies $\mathbf{P}^H\mathbf{R}_i\mathbf{P} \cong \mathbf{R}_i$. So we have the approximate equation $\mathbf{P}^H\hat{\mathbf{R}}_i\mathbf{P} \cong \hat{\mathbf{R}}_i$. Combine (26) and (27), we have:

$$\mathbf{P}^H\hat{\mathbf{R}}\mathbf{P} - \hat{\sigma}_n^2\mathbf{P}^H\mathbf{P} \cong \hat{\mathbf{R}}_i \tag{28}$$

The terms of $\mathbf{P}^H\hat{\mathbf{R}}\mathbf{P} - \hat{\sigma}_n^2\mathbf{P}^H\mathbf{P}$ preserves the interference components. However, the projection operation may cause lots of errors. Thus we aim to estimate the powers of each interference from $\mathbf{P}^H\hat{\mathbf{R}}\mathbf{P} - \sigma_n^2\mathbf{P}^H\mathbf{P}$ instead of regarding it as ICM. The theoretical $\mathbf{R}_i$ is expressed in (6):

$$\mathbf{R}_i = \sum_{l=1}^{L}\sigma_l^2\mathbf{a}_l\mathbf{a}_l^H = \mathbf{A}_i\Lambda_i\mathbf{A}_i^H \tag{29}$$

where $\mathbf{A}_i = [\mathbf{a}_1, \mathbf{a}_2, \cdots, \mathbf{a}_L] \in \mathbb{C}^{M\times L}$ represents the SVs of interference. $\Lambda_i = diag\{\sigma_1^2, \sigma_2^2, \cdots, \sigma_L^2\}$ is diagonal matrix and each elements stands for the powers of corresponding interference. In order to obtain the Λ_i, we pre-multiply the above equation by $(\mathbf{A}_i^H\mathbf{A}_i)^{-1}\mathbf{A}_i^H$ and post-multiply the above equation by $\mathbf{A}_i(\mathbf{A}_i^H\mathbf{A}_i)^{-1}$, then we have:

$$\Lambda_i = (\mathbf{A}_i^H\mathbf{A}_i)^{-1}\mathbf{A}_i^H\mathbf{R}_i\mathbf{A}_i(\mathbf{A}_i^H\mathbf{A}_i)^{-1} \tag{30}$$

The above equation is explained as: if we have the SVs of interference and the ICM, we can express the powers of interference as a diagonal matrix. We can replace $\mathbf{R}_i$ by $\hat{\mathbf{R}}_i$ in (26). For $\mathbf{A}_i$, there are multiply spectrum peaks by performing searching in the space through (13) in [23]. From the locations of peaks, we get the direction estimators $\{\bar{\theta}_1, \bar{\theta}_2 \cdots, \bar{\theta}_{\hat{L}}\}$, and combine the known array geometry, we obtain the corresponding SVs $\{\bar{\mathbf{a}}(\bar{\theta}_1), \bar{\mathbf{a}}(\bar{\theta}_2), \cdots, \bar{\mathbf{a}}(\bar{\theta}_{\hat{L}})\} = \{\bar{\mathbf{a}}_1, \bar{\mathbf{a}}_2, \cdots, \bar{\mathbf{a}}_{\hat{L}}\} = \tilde{\mathbf{A}}_i$. So the estimated powers of interference is expressed as:

$$\tilde{\Lambda}_i = (\tilde{\mathbf{A}}_i^H\tilde{\mathbf{A}}_i)^{-1}\tilde{\mathbf{A}}_i^H(\mathbf{P}^H\hat{\mathbf{R}}\mathbf{P} - \hat{\sigma}_n^2\mathbf{P}^H\mathbf{P})\tilde{\mathbf{A}}_i(\tilde{\mathbf{A}}_i^H\tilde{\mathbf{A}}_i)^{-1} \tag{31}$$

where $\tilde{\Lambda}_i \in \mathbb{C}^{\hat{L}\times\hat{L}}$ is not diagonal matrix which is different from Λ, while the diagonal elements of $\tilde{\Lambda}_i$ represent the corresponding powers of interference. The term of $\mathbf{P}^H\hat{\mathbf{R}}\mathbf{P} - \hat{\sigma}_n^2\mathbf{P}^H\mathbf{P}$ is absent of desired signal components, which can reduce the estimation errors and is quite different from previous interference powers estimation methods like [23]. Although $\mathbf{P}^H\hat{\mathbf{R}}\mathbf{P} - \hat{\sigma}_n^2\mathbf{P}^H\mathbf{P}$ contains some error components, it doesn't affect the interference powers estimation seriously. Then we reconstruct the INCM based on the powers of interference and corresponding SVs:

$$\tilde{\mathbf{R}}_{i+n} = \tilde{\mathbf{A}}_i\mathbf{diag}(\tilde{\Lambda}_i)\tilde{\mathbf{A}}_i^H + \hat{\sigma}_n^2\mathbf{I} \tag{32}$$

where $\mathbf{diag}(\tilde{\Lambda}_i)$ means that get the diagonal elements of $\tilde{\Lambda}_i$ and turn it into a new diagonal matrix. Substituting $\hat{\mathbf{a}}_s$ and $\tilde{\mathbf{R}}_{i+n}$ into (8), the proposed beamformer is designed as:

$$\mathbf{w}_{pro} = \frac{\tilde{\mathbf{R}}_{i+n}^{-1}\hat{\mathbf{a}}_s}{\hat{\mathbf{a}}_s^H\tilde{\mathbf{R}}_{i+n}^{-1}\hat{\mathbf{a}}_s} \tag{33}$$

In proposed method, the computational complexity of desired signal SV estimation is $O(M^2S + M^3)$ including integration operation and Eigen decomposition, where S is

the number of sampling points in Θ_s. In ICM reconstruction part, the spectrum searching and matrix inverse operation are $O(M^2Q + M^3)$, where Q denotes the number of searching points. Compared with [18], [19], [22], the proposed method is more efficient.

Based on the above description, the proposed algorithm is summarized as follows:

Algorithm 1 Proposed RAB Algorithm

1: Calculated the sample covariance matrix $\hat{\mathbf{R}}$ and obtain the Capon power spectrum (13).
2: Estimate the residual noise power $\bar{\sigma}^2$ using (19) and calculate the actual noise power $\hat{\sigma}^2$ via (20).
3: Reconstruct $\hat{\mathbf{R}}_s$ using (22) and eigen-decompose $\hat{\mathbf{R}}_s$ to obtain the $\hat{\mathbf{a}}_s$ and $\mathbf{C}_1$.
4: Compute the covariance matrix $\tilde{\mathbf{R}}$ via (27) and $\hat{\mathbf{R}}_i$ via (28).
5: Obtain the interference SVs $\tilde{\mathbf{A}}_i$ via (13) and calculate the interference powers based on (31).Then reconstruct $\tilde{\mathbf{R}}_{i+n}$ via (32).
6: Obtain the weight vector of proposed algorithm $\mathbf{w}_{pro}$ (33).

IV. SIMULATION RESULTS

In our simulations, a uniform linear array with $M = 10$ omnidirectional sensors spaced half a wavelength is considered. There are three signals impinging from the directions $\theta_0 = -5°$, $\theta_1 = -40°$ and $\theta_2 = 30°$, and the estimated directions are $\bar{\theta}_0 = -8°$, $\bar{\theta}_1 = -43°$, $\bar{\theta}_2 = 27°$. The first signal is assumed to be the desired signal and the other two signals are interference with 20 dB interference-to-noise-ratios (INR). The additive noise is modeled as a Gaussian zero-mean spatial and temporal white process. The angular region of one desired signal and two interference are set to be $\Theta_0 = [\bar{\theta}_0 - 8°, \bar{\theta}_0 + 8°]$, $\Theta_1 = [\bar{\theta}_1 - 8°, \bar{\theta}_1 + 8°]$ and $\Theta_2 = [\bar{\theta}_2 - 8°, \bar{\theta}_2 + 8°]$ respectively, while the complement angular sectors of Θ_0 is $\bar{\Theta}_0 = [-90°, \bar{\theta}_0 - 8°) \bigcup (\bar{\theta}_0 + 8°, 90°]$ and the interference angular sector is $\Theta_i = \Theta_1 \bigcup \Theta_2$. All integral operations in this paper are replaced by discrete sums and all angular sectors are uniformly sampled to be discrete sectors with the same angular interval $\Delta\theta = 0.1°$. For each scenario, 200 Monte-Carlo runs are performed.

The proposed method is compared to the eigen-based (EIG) beamformer [12], the worst-case-based beamformer (WCP) [13], the linear reconstruction-based beamformer (INCM-linear) [18], the volume reconstruction-based beamformer (INCM-volume) [19], the spatial power spectrum sampling beamformer (INCM-SPSS) [20] and the subspace reconstruction-based beamformer (INCM-subspace) [22]. We assume that the parameter $\rho = 0.9$ for both [12] and [22], the uncertainty set parameter $\varepsilon = 0.3M$ for [13] and the parameter $\varepsilon = \sqrt{0.1}$ for [19]. The $\alpha_0 = 0°$ is used and $\delta = sin^{-1}(M/2)$ in [20]. The parameter $N = 3$ is set in proposed method to determine the dominant eigenvectors of $\mathbf{C}_1$. Convex optimization toolbox CVX [27] is used to solve optimization problems.

Example 1 (Mismatch Due to Look Direction Error): In the first example, assume that the random direction errors of desired signal and interference are uniformly distributed in $[-4°, 4°]$ for each simulation. Fig. 3 demonstrates the output SINR curves of tested methods versus the input SNR for the fixed snapshot $K = 30$. It shows that the proposed method and INCM-reconstruction beamformers [18]–[20], [22] achieve better performance than EIG [12] and WCP beamformers [13]. Fig. 4 denotes the deviation from optimal output SINR curves of proposed method and INCM-reconstruction methods [18]–[20], [22], and we can see that the proposed method acquires the least deviation. Although the curves of INCM-subspace beamformer is close to the proposed method, the proposed method has the lower computational complexity. The proposed method strongly benefits the high accurate estimations of both the desired signal SV and ICM. It's well

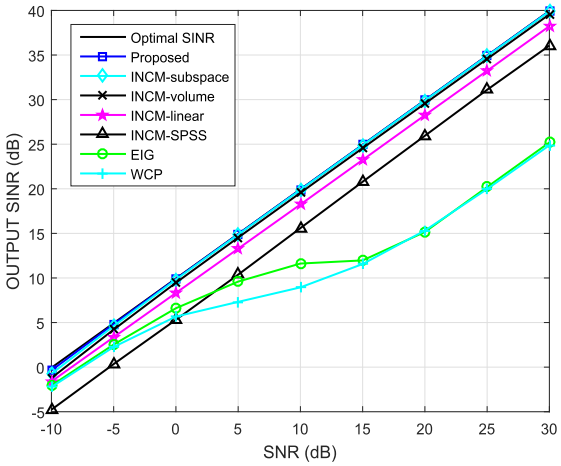

FIGURE 3. Output SINR versus the input SNR in case of look direction error.

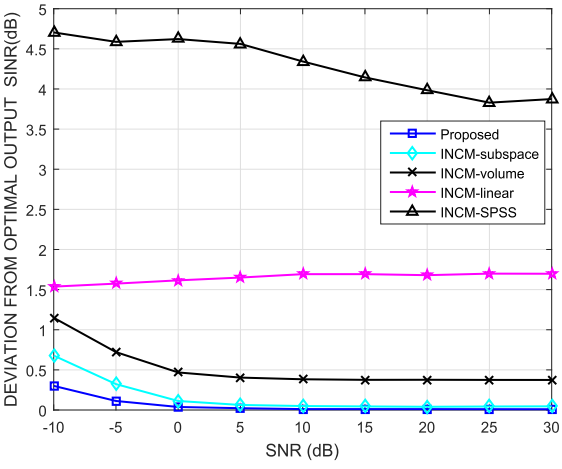

FIGURE 4. Deviation from optimal SINR versus input SNR in case of look direction error.

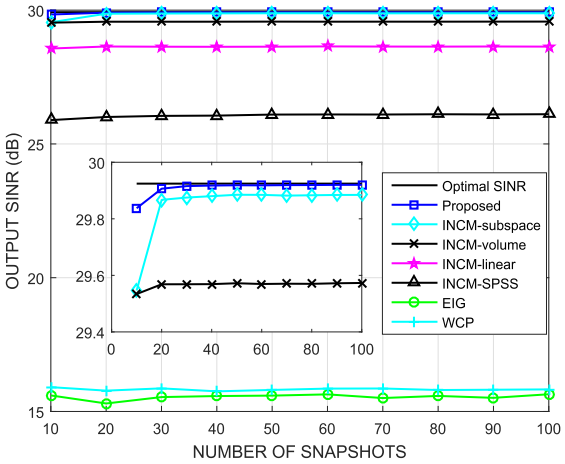

FIGURE 5. Output SINR versus the number of snapshots in case of look direction error.

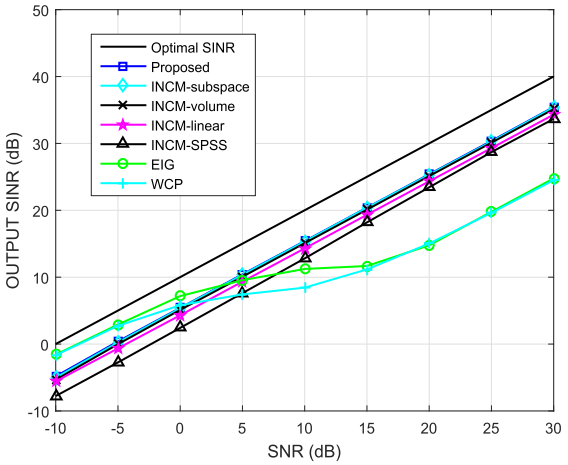

FIGURE 6. Output SINR versus the input SNR in case of Amplitude and Phase Perturbations.

known that the theoretical ICM is a linear combination of the SVs and powers of interferences, and the reconstructed ICM in proposed method is the linear combination of estimated powers $\tilde{\Lambda}_i$ and corresponding SVs $\tilde{\mathbf{A}}_i$. Compared with INCM-reconstruction methods [18], [19], INCM-volume [19] beamformer achieves the better performance. That is because the INCM-volume uses an annulus uncertainty set to constrain the SVs of interference and integrates the Capon spectrum over the surface of annulus. Fig. 5 shows the curves of output SINR versus the number of snapshots at SNR $=$ 20 dB. Clearly, the proposed method and INCM-subspace beamformer [22] almost get the optimal performance. Due to the proposed method is based on the interference powers estimation and doesn't suffer from the influence of desired signal, it has the best performance of tested beamformers.

Example 2 (Mismatch Due to Amplitude and Phase Perturbations Error): In the second example, the influence of amplitude and phase perturbations on output SINR is taken into consideration. Assuming that the amplitude and phase errors of each sensor are Gaussian distributions $N(1, 0.1^2)$ and $N(1, (0.25\pi)^2)$, respectively. Fig. 6 corresponds to the output SINR curves versus the input SNR at the condition $K = 30$. The proposed method almost attains the best performance no matter in low or high input SINR, and when the input SNR is lower than 0dB, the EIG [12] and WCP [13] beamformers perform better than INCM beamformers [18]–[20], [22]. Fig. 7 draws the curves of deviation from optimal output SINR of proposed method and INCM-reconstruction methods [18]–[20], [22]. The proposed method has the higher output SINR than INCM-subspace [22] because there is a obvious gap between them, besides, the proposed method doesn't need eigen-decomposition for each SV of interference like [22]. The true SV of desired signal must belong to the signal subspace. In proposed method, we reconstruct the desired signal covariance matrix based on the accurate power spectrum which doesn't contain the residual noise,

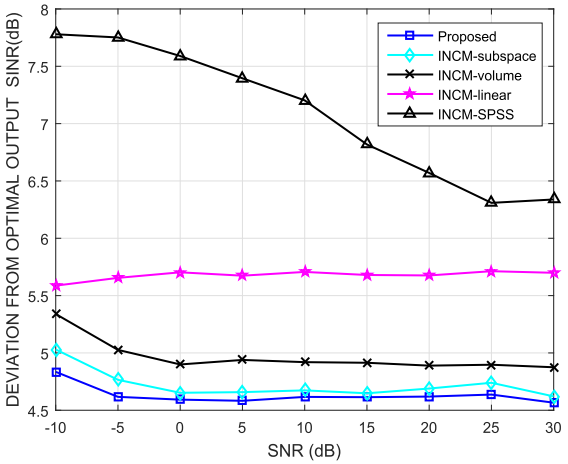

FIGURE 7. Deviation from optimal SINR versus the input SNR in case of Amplitude and Phase Perturbations.

and the corresponding eigenvectors span the signal subspace. Thus, we choose the eigenvector corresponding the largest eigenvalue as the estimated desired signal SV. Fig. 8 depicts the output SINR curves versus the number of snapshots in the condition of SNR $=$ 20 dB. Although the curves of all tested beamformers have deviations from optimal output SINR, the proposed method outperform the other beamformers and reaches the highest output SINR. The results strongly demonstrate that the proposed method has the better estimation of the desired signal SV and ICM because the estimated desired signal doesn't suffer from the influence of residual noise and the reconstructed ICM doesn't suffer from the influence of desired signal. From Fig. 8, we can also conduct that the number of snapshots doesn't influence the performance of proposed method.

Example 3 (Mismatch Due to SV Random Error): In this example, the SVs of desired signal and interference are assumed to be randomly distributed in an uncertainty set that

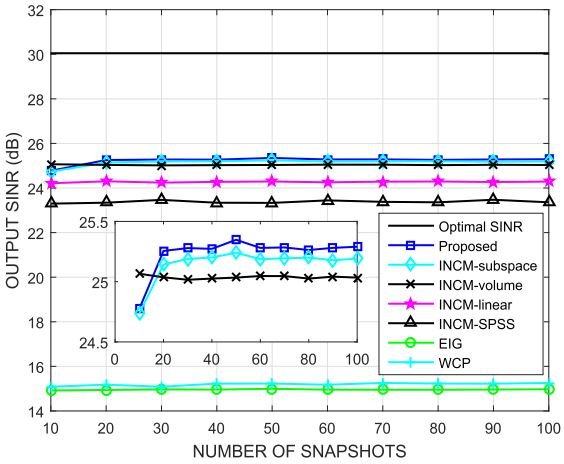

FIGURE 8. Output SINR versus the number of snapshots in case of Amplitude and Phase Perturbations.

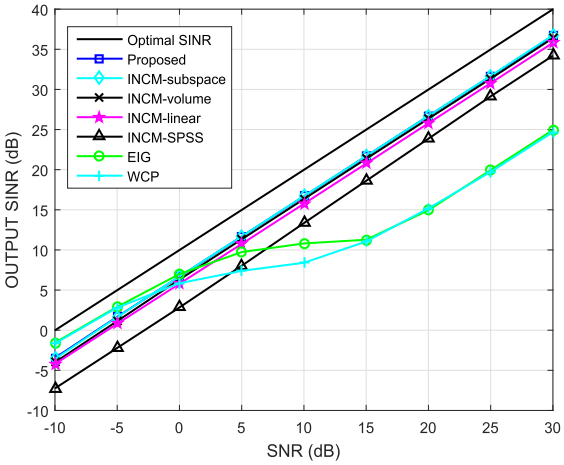

FIGURE 9. Output SINR versus the input SNR in case of SV random error.

can be modeled as:

$$\mathbf{a}_l = \bar{\mathbf{a}}_l + \mathbf{e}_l, \quad l = 0, 1, \cdots, L \tag{34}$$

where $\bar{\mathbf{a}}_l$ stands for the nominal SV corresponding to the direction $\bar{\theta}_l$, and $\mathbf{e}_l$ represents the random error vector. The random error vector can be written as follow:

$$\mathbf{e}_l = \frac{\varepsilon_l}{\sqrt{M}}[e^{j\phi_0^l}, e^{j\phi_1^l}, \cdots, e^{j\phi_{M-1}^l}]^T \tag{35}$$

where ε_l denotes the norm of $\mathbf{e}_l$ and it's uniformly distributed in the interval $[0, \sqrt{0.3}]$ in each simulation run. $\phi_m^l, m = 0, 1, \cdots, M-1$ represents the phases of random error vector $\mathbf{e}_l$, which is independently and uniformly distributed in $[0, 2\pi)$. The mismatch in (34) is comprehensive which is considered to contain direction errors, calibration errors and so on. Fig. 9 illustrates the output SINR curves versus the input SNR for the number of snapshots $K = 30$, and the proposed method and INCM beamformers [18], [19], [22] almost have the same output SINR. From Fig. 10 which displays the curves of deviation from optimal output SINR, it's clear seen that the

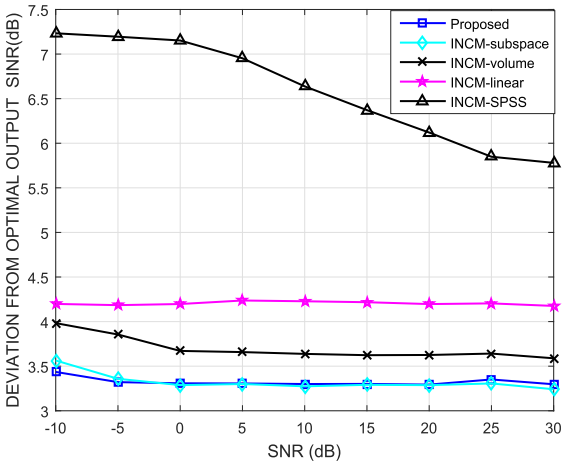

FIGURE 10. Deviation from optimal SINR in case of SV random error.

proposed method obtains the highest output SINR as INCM-subspace [22] of all tested beamformers. Compared with proposed method and INCM-subspace [22], the differences are the INCM-subspace [22] method searches for the SV lying in insertion of two subspace, while the proposed method searches for the SV based on the peaks of power spectrum distribution and the known array geometry, and the interference powers estimation of proposed method doesn't suffer from the influence of desired signal. Besides, the reconstructed ICM in proposed method has the same formulation as theoretical definition. Based on the similar performance of proposed method and [22], the proposed method is more efficient than INCM-subapce [22] beamformer. Compared with INCM-volume [19], INCM-linear [18] and INCM-SPSS [20] beamformers, the reconstructed INCM in [18], [19] collects lots of residual noise components, and in INCM-SPSS [20] beamformer, the reconstructed INCM still includes the desired signal components. Fig. 11 draws the output SINR versus the number of snapshots at SNR = 20 dB. The results demonstrate that the number of snapshots doesn't affect the output SINR seriously and the proposed method get the best performance of all tested beamformers.

Example 4 (Mismatch Due to Incoherent Local Scattering Error): In the fourth example, we analyze the influence of incoherent local scattering on output SINR. Assuming that the desired signal has a time-varying spatial signature that is different for each data snapshot, which is modeled as:

$$\mathbf{x}(k) = s_0(k)\mathbf{a}_0 + \sum_{p=1}^{4} s_p(k)\bar{\mathbf{a}}(\theta_p') \tag{36}$$

where $\mathbf{a}_0$ represents the SV of desired signal impinging from the direction $\theta_0 = 0°$, $\bar{\mathbf{a}}(\theta_p'), p = 1, 2, 3, 4$ denotes the SV of the incoherent scattering signals. The directions $\theta_p', p = 1, 2, 3, 4$ are independently and randomly drawn from the Gaussian generator $N(\theta_0, 4°)$. $s_0(k)$ and $s_p(k), p = 1, 2, 3, 4$ are independently and identically distributed complex Gaussian random variables drawn from the random generator

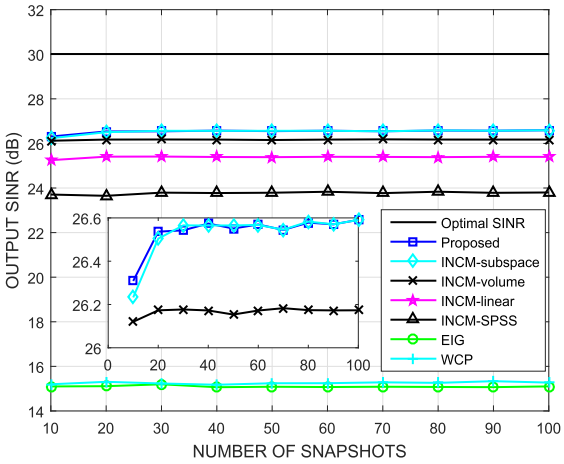

FIGURE 11. Output SINR versus the number of snapshots in case of SV random error.

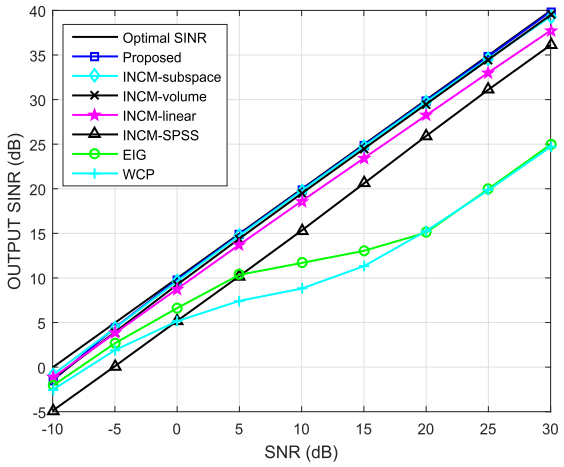

FIGURE 12. Output SINR versus the input SNR in case of incoherent local scattering error.

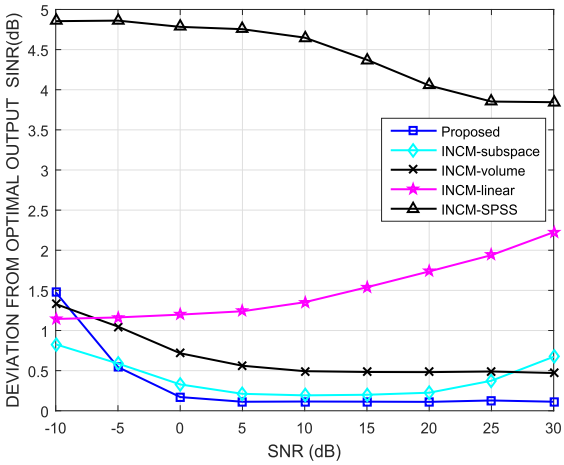

FIGURE 13. Deviation from optimal SINR in case of incoherent local scattering error.

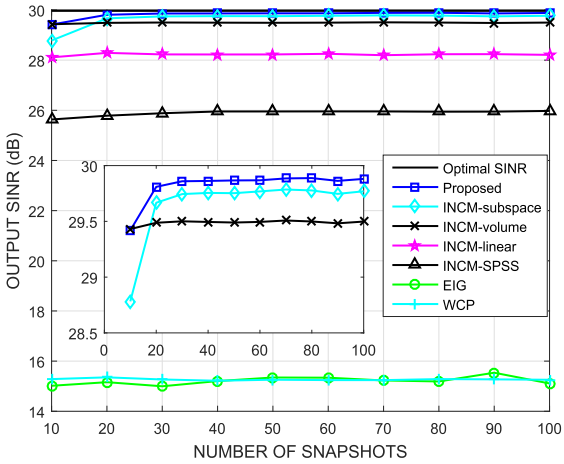

FIGURE 14. Output SINR versus the number of snapshots in case of incoherent local scattering error.

$N(0, 1)$. Different from previous examples, the desired signal covariance matrix is no longer a rank-one matrix and the output SINR should be expressed as [7]:

$$SINR_{opt} = \frac{\mathbf{w}^H \mathbf{R}_s \mathbf{w}}{\mathbf{w}^H \mathbf{R}_{i+n} \mathbf{w}} \tag{37}$$

then the optimal weight vector can be obtained by maximizing the SINR:

$$\mathbf{w}_{opt} = \mathcal{P}\{\mathbf{R}_{i+n}^{-1} \mathbf{R}_s\} \tag{38}$$

where $\mathcal{P}$ denotes the principal eigenvector corresponding to the largest eigenvalue of the matrix. Fig. 12 displays the output SINR curves versus the input SNR for the fixed number of snapshots $K = 30$, and no matter in low or high input SINR, the performance of proposed method is better than all tested beamformers. Fig. 13 demonstrates the deviation from optimal output SINR of tested beamformers. When the input SNR is large than 25 dB, the deviation between proposed method and INCM-subspace [22] is more than 0.5 dB. The superior performance of performance due to the accurate estimation of desired signal SV and ICM. We remove the residual noise components from Capon power spectrum to reconstruct the desired signal covariance matrix, and the eigenvector corresponding to largest eigenvector contains the most information which is regarded as the SV. For interference powers estimation, we project the snapshot onto the complementary subspace of desired signal to reduce the estimation errors. Fig. 14 depicts the output SINR curves versus the number of snapshots on the condition of SNR = 20 dB. When the snapshots are less than 30, there is the significant deviation between proposed method and INCM-subspace [22] beamformer, and the proposed method almost achieves the optimal performance no matter in large or small number of snapshots.

The above four simulation examples have proved that the proposed method is robust to achieve satisfactory performance against various mismatch errors. In the cases of direction error and incoherent local scattering error, the proposed method almost get the optimal output SINR, and in the cases

of amplitude and phase perturbations error and SV random error, although there is a gap between the curves of optimal output SINR and proposed method, the proposed method still outperforms the existing beamformers.

V. CONCLUSION

In this paper, we develop the RAB approach based on the residual noise elimination and interference power estimation for covariance matrix reconstruction. The proposed method first analyzes the existence of residual noise and its relationship to actual noise. Based on this, we obtain the accuracy power spectrum distribution to reconstruct the desired signal covariance matrix, and the principle eigenvector is employed as desired signal SV. For ICM reconstruction, we project the snapshots onto complementary subspace of desired signal to reduce the influence of desired signal on interference powers estimation, and the estimated interference powers are derived from the theoretical formulation of ICM. Then we reconstruct the ICM like theoretical definition. Simulation results demonstrate that the proposed method is robust against many types of mismatch errors and attains excellent performance of tested beamformers.

REFERENCES

[1] J. Capon, "High-resolution frequency-wavenumber spectrum analysis," *Proc. IEEE*, vol. 57, no. 8, pp. 1408–1418, Aug. 1969.

[2] S. Shahbazpanahi, A. B. Gershman, Z.-Q. Luo, and K. M. Wong, "Robust adaptive beamforming for general-rank signal models," *IEEE Trans. Signal Process.*, vol. 51, no. 9, pp. 2257–2269, Sep. 2003.

[3] A. M. Vural, "Effects of perturbations on the performance of optimum/adaptive arrays," *IEEE Trans. Aerosp. andElectron. Syst.*, vol. AES-15, no. 1, pp. 76–87, Jan. 2007.

[4] B. D. Carlson, "Covariance matrix estimation errors and diagonal loading in adaptive arrays," *IEEE Trans. Aerosp. Electron. Syst.*, vol. 24, no. 4, pp. 397–401, Jul. 1988.

[5] J. Li, P. Stoica, and Z. Wang, "On robust Capon beamforming and diagonal loading," *IEEE Trans. Signal Process.*, vol. 51, no. 7, pp. 1702–1715, Jul. 2003.

[6] A. Elnashar, S. M. Elnoubi, and H. A. El-Mikati, "Further study on robust adaptive beamforming with optimum diagonal loading," *IEEE Trans. Antennas Propag.*, vol. 54, no. 12, pp. 3647–3658, Dec. 2006.

[7] L. Du, J. Li, and P. Stoica, "Fully automatic computation of diagonal loading levels for robust adaptive beamforming," *IEEE Trans. Aerosp. Electron. Syst.*, vol. 46, no. 1, pp. 449–485, Jan. 2010.

[8] D. D. Feldman and L. J. Griffiths, "A projection approach for robust adaptive beamforming," *IEEE Trans. Signal Process.*, vol. 42, no. 4, pp. 867–876, Apr. 1994.

[9] D. D. Feldman, "An analysis of the projection method for robust adaptive beamforming," *IEEE Trans. Antennas Propag.*, vol. 44, no. 7, pp. 1023–1030, Jul. 1996.

[10] F. Huang, W. Sheng, and X. Ma, "Modified projection approach for robust adaptive array beamforming," *Signal Process.*, vol. 92, no. 7, pp. 1758–1763, Jul. 2012.

[11] J. Zhuang and A. Manikas, "Interference cancellation beamforming robust to pointing errors," *IET Signal Process.*, vol. 7, no. 2, pp. 120–127, Apr. 2013.

[12] W. Jia, W. Jin, S. Zhou, and M. Yao, "Robust adaptive beamforming based on a new steering vector estimation algorithm," *Signal Process.*, vol. 93, no. 9, pp. 2539–2542, Sep. 2013.

[13] S. A. Vorobyov, A. B. Gershman, and Z.-Q. Luo, "Robust adaptive beamforming using worst-case performance optimization: A solution to the signal mismatch problem," *IEEE Trans. Signal Process.*, vol. 51, no. 2, pp. 313–324, Feb. 2003.

[14] J. Li, P. Stoica, and Z. Wang, "Doubly constrained robust capon beamformer," *IEEE Trans. Signal Process.*, vol. 52, no. 9, pp. 2407–2423, Sep. 2004.

[15] R. G. Lorenz and S. P. Boyd, "Robust minimum variance beamforming," *IEEE Trans. Signal Process.*, vol. 53, no. 5, pp. 1684–1696, May 2005.

[16] S. E. Nai, W. Ser, Z. L. Yu, and H. Chen, "Iterative robust minimum variance beamforming," *IEEE Trans. Signal Process.*, vol. 59, no. 4, pp. 1601–1611, Apr. 2011.

[17] A. Khabbazibasmenj, S. A. Vorobyov, and A. Hassanien, "Robust adaptive beamforming based on steering vector estimation with as little as possible prior information," *IEEE Trans. Signal Process.*, vol. 60, no. 6, pp. 2974–2987, Jun. 2012.

[18] Y. Gu and A. Leshem, "Robust adaptive beamforming based on interference covariance matrix reconstruction and steering vector estimation," *IEEE Trans. Signal Process.*, vol. 60, no. 7, pp. 3881–3885, Jul. 2012.

[19] L. Huang, J. Zhang, X. Xu, and Z. Ye, "Robust adaptive beamforming with a novel interference-plus-noise covariance matrix reconstruction method," *IEEE Trans. Signal Process.*, vol. 63, no. 7, pp. 1643–1650, Apr. 2015.

[20] Z. Zhang, W. Liu, W. Leng, A. Wang, and H. Shi, "Interference-plus-noise covariance matrix reconstruction via spatial power spectrum sampling for robust adaptive beamforming," *IEEE Signal Process. Lett.*, vol. 23, no. 1, pp. 121–125, Jan. 2015.

[21] F. Shen, F. Chen, and J. Song, "Robust adaptive beamforming based on steering vector estimation and covariance matrix reconstruction," *IEEE Commun. Lett.*, vol. 19, no. 9, pp. 1636–1639, Sep. 2015.

[22] X. Yuan and L. Gan, "Robust adaptive beamforming via a novel subspace method for interference covariance matrix reconstruction," *Signal Process.*, vol. 130, pp. 233–242, Jan. 2017.

[23] Z. Zheng, Y. Zheng, W.-Q. Wang, and H. Zhang, "Covariance matrix reconstruction with interference steering vector and power estimation for robust adaptive beamforming," *IEEE Trans. Veh. Technol.*, vol. 67, no. 9, pp. 8495–8503, Sep. 2018.

[24] H. L. van Trees, *Optimum Array Processing: Part IV of Detection, Estimation, and Modulation Theory*. Hoboken, NJ, USA: Wiley, 2002, pp. 428–709.

[25] P. Stoica, J. Li, and X. Tan, "On spatial power spectrum and signal estimation using the pisarenko framework," *IEEE Trans. Signal Process.*, vol. 56, no. 10, pp. 5109–5119, Oct. 2008.

[26] R. A. Horn, R. A. Horn, and C. R. Johnson, *Matrix Analysis*. Cambridge, U.K.: Cambridge Univ. Press, 1990.

[27] M. Grant and S. Boyd, "Cvx: Matlab software for disciplined convex programming, version 1.21," *Global Optim.*, vol. 5, pp. 155–210, Oct. 2008.

XINGYU ZHU received the B.Eng. degree in electronic and information engineering from the Hefei University of Technology, Hefei, China, in 2017. He is currently pursuing the M.Eng. degree with the University of Science and Technology of China, Hefei. His research interest includes array signal processing, especially the robust adaptive beamforming.

ZHONGFU YE received the B.Eng. and M.S. degrees in electronic and information engineering from the Hefei University of Technology, Hefei, China, in 1982 and 1986, respectively, and the Ph.D. degree from the University of Science and Technology of China, Hefei, China, in 1995, where he is currently a Professor. His current research interests are in statistical and array signal processing, speech processing, and image processing.

XU XU received the B.E. degree in electronic engineering from the Hefei University of Technology, Hefei, China, in 1997, and the M.S. degree in communication and information system from the University of Science and Technology of China, Hefei, in 2000, where she has been a Teacher with the Department of Electronic Engineering and Information Science, since 2000. Her current research interest is in array signal processing.

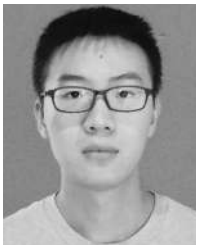

RUI ZHENG received the B.Eng. degree in electronic information engineering from Jiangsu University, Zhenjiang, China, in 2017. He is currently pursuing the M.Eng. degree in electronics and communication engineering with the University of Science and Technology of China, Hefei, China. His research interests include sparse representation, convex optimization theory, and array signal processing.